Numerical Simulation of the Effect of Finite Diaphragm Rupture Process on Micro Shock Tube Flows

Arun Kumar R* and Heuy Dong Kim*†

ABSTRACT

Recent years have witnessed the use of micro shock tube in various engineering applications like micro combustion, micro propulsion, particle delivery systems etc. The flow characteristics occurring in the micro shock tube shows a considerable deviation from that of well established conventional macro shock tube due to very low Reynolds number and high Knudsen number effects. Also the diaphragm rupture process, which is considered to be instantaneous process in many of the conventional shock tubes, will be crucial for micro shock tubes in determining the near diaphragm flow field and shock formation. In the present study, an axi-symmetric CFD method has been applied to simulate the micro shock tube, with Maxwell's slip velocity and temperature jump boundary conditions. The effects of finite diaphragm rupture process on the flow field and the shock formation was investigated, in detail. The results show that the shock strength attenuates rapidly as it propagates through micro shock tubes.

Key Words : Diaphragm Rupture, Expansion Wave, Micro Shock Tube, Rarefaction, Unsteady Flow.

1. INTRODUCTION

Recent years have seen the implementation of micro shock tube in various emerging technologies like micro heat engines, micro propulsion, needleless injection devices etc. Micro shock tubes which are functionally similar to macro shock tubes consist of driver section and driven section which are separated by a diaphragm or a quickly opening valve. Sudden rupture of the diaphragm initiates unsteady flow from the driver section at a high pressure to the driven section at a relatively low pressure. The extreme low flow dimensions for a micro shock tube reduces the Reynolds number and cause an increase in Knudsen number. It is well known that as the Knudsen number increases the molecular forces becomes predominant in controlling the flow physics. These flow situations leads to rarefaction effects which cause the wall attached fluid to slip rather attaching to wall.

Owing to these disparities in flow physics, the conventional macro shock tube understanding is not sufficient enough to predict the shock propagation and associated

* School of Mechanical Engineering, Andong National University
† Corresponding author: Heuy Dong Kim
E-mail: kimhd@andong.ac.kr

flow field for a micro shock tube.

Due to very small flow dimension micro shock tube exhibits very large surface area to volume ratio. This causes the boundary layer thickness and associated viscous losses to greatly influence the shock propagation. This has been observed by Duff [1] through his experimental studies on a small shock tube of 28.6 mm diameter. He also observed that the shock strength is much influenced by the initial pressure. Hence a lower initial pressure causes much attenuation of shock. Later Brouillette [2] devised a scaling factor for micro shock tube flows, which relates the diameter and initial pressure to the shock attenuation. Moreover as the initial operating pressure reduces the molecular mean free path increases and eventually increases the Knudsen Number (Kn), which is the ratio between the mean free path to flow diameter. Most of the micro shock tube flows, due to its inherent low diameter and low operating pressure, have a Knudsen number ranging between 0.01 to 0.1 which causes rarefaction effects and makes the near wall fluid to slip and an elevated temperature at the wall attached fluid. These properties alter the boundary layer effects and bring additional disparities to the shock flow field. A numerical study to investigate the shock propagation under slip condition was carried out by Zeitoun [3].He also investigated molecular dynamics simulation [4] to improve the accuracy of shock propagation prediction in micro shock tubes, which becomes significant at flows having Kn greater than 0.1.

Most of the shock tube studies done in the past assumed an instantaneous diaphragm rupture process. But in actual scenario the diaphragm opens with a finite rupture time. This causes complex 2D flows near the diaphragm and a series of compression waves will be generated subsequent to finite opening steps and eventually will yield to shock waves. It is hard to derive some mathematical models to match the diaphragm opening process. Shigeru Matsuo [5] did an experimental analysis to determine the diaphragm rupture time at different low pressure ratios. They constructed the expansion head wave and expansion tail wave along the driver section. Because of a finite opening time these to loci will not meet at origin, which is the diaphragm position, but will produce an imaginary center downstream of the diaphragm for the non centered expansion wave and the gap between the loci of head and tail was considered to be the diaphragm opening time. The experimental setup details are shown in Fig.1.

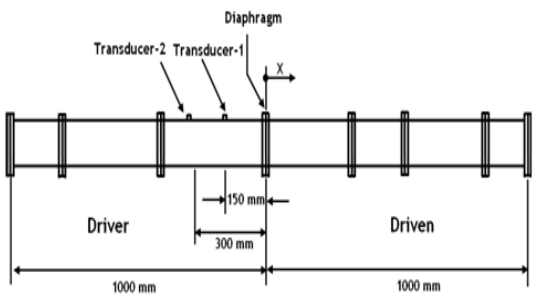

Fig. 1 Schematic diagram for the experimental setup

The phenomenon of diaphragm rupture is a highly complicated three-dimensional process. In the above experimental work the authors suggested a quadratic function to imitate the diaphragm rupture process. Another model which uses a cosine function for the diaphragm opening area with respect to opening time was proposed by Outa [6].

In the past there have been some studies to understand the effect of diaphragm rupture

process on macro shock tubes [7,8,9].But in the case of micro shock tubes the unsteady shock evolution and the associated flow field with a finite diaphragm rupture process is even more complicated due to the slip and boundary layer effects. In the present study a 2D axi-symmetric CFD approach was used to simulate the unsteady flow evolution and shock propagation inside a micro shock tube considering the diaphragm rupture process.

2. NUMERICAL SIMULATION

For the present study an axi-symmetric shock tube model of 1mm diameter was considered as shown below.

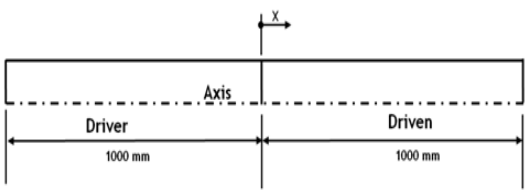

Fig. 2 Schematic diagram for micro shock tube (ϕ1 mm)

The determination of diaphragm rupture time for a micro shock tube is extremely hard due to very small rupture time scale and experimental difficulties due to very small flow dimensions. Few years back, Shigeru Matsuo experimentally found out the diaphragm rupture time for a macro shock tube of 65.5 mm diameter under various low pressure ratios as discussed in the above section and the experimental diaphragm opening results are shown in Fig.3

From this experimental result of conventional macro shock tube the diaphragm

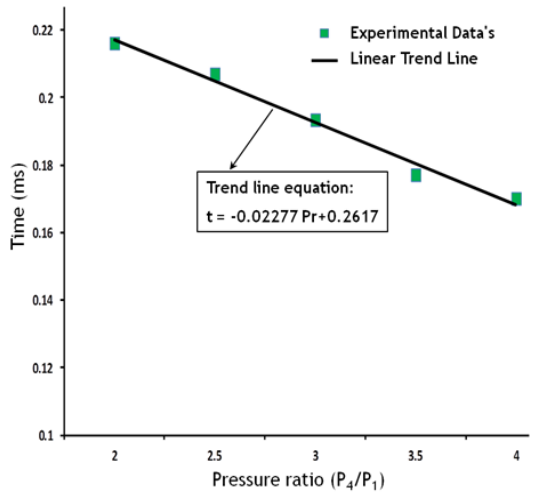

Fig. 3 Experimental diaphragm opening time at various pressure ratios

rupture time for a micro shock tube of 1mm diameter and at low initial pressure can be found by using some interpolation techniques as explained below.

The diaphragm rupture time mainly depends on three factors:

1. Diaphragm area,
2. Net pressure (P4-P1) acting across the diaphragm
3. Diaphragm thickness

The experimental result (Fig.3) at the minimum pressure ratio (Pr=2; P4=101300 Pa;P1=50650 Pa) gives a rupture time of 0.216 ms. The net rupture force for this case will be 50650 Pa. But for studying the slip effects on shock propagation the numerical study should be carried out at a much lower operational pressure. It can be noted that the same net pressure can be obtained at a much lower initial pressures (P4=51161 Pa; P1-511.61 Pa) but with a higher pressure ratio of 100.For the latter case also the diaphragm rupture time will be 0.216 ms since the diaphragm area, net pressure force and diaphragm thickness

remained unaltered. But this low pressure produces a Knudsen number of 0.01at the driven section, which is in the verge of no slip wall conditions and hence not suitable for studying the rarefaction effect on shock propagation.

From the above experimental results it can be observed that the diaphragm rupture time shows linear trend, as t = -0.02277 Pr+0.2617, with respect to pressure ratio. It can also be noted that a lower pressure ratio yields a low net pressure force in which case a much lower initial operating pressure can be considered. For this purpose opening time at a pressure ratio of 1.4 was found based on the linear trend. The net force acting across the diaphragm for this case (Pr=1.4; P4=101300 P1=72357 Pa) will be 28942 Pa. The same net pressure force can be achieved with a lower driver and driven pressure of 29235 Pa and 292.35 Pa respectively but with a higher pressure ratio of 100.The very low pressure in the driven tube makes the Knudsen number to 0.025 and the flow will fall under slip conditions. The diaphragm opening time based on the linear trend line equation will be 0.2296ms.This time is for shock tube of 65.5mm diameter. Assuming a direct relationship of diaphragm rupture time with area, the rupture time for a 1 mm tube can be easily found out and is about 0.053 μs.

The total diaphragm opening time was divided into 30 discrete time steps and the diaphragm opening radius at each time step is found based on some assumed opening functions with respect to time as shown in below equations.

Linear Opening:

$$r = 9.931 \times t \qquad (1)$$

Cosine Opening (by Outa [6]):

$$\frac{d^2}{D^2} = 1 - \cos\left(\frac{\pi}{2}\left(\frac{t - t_r}{T}\right)^2\right) \qquad (2)$$

Quadratic Opening (Shigeru Matsuo):

$$t = \left(\left(\frac{r}{R}\right)^2 T\right) \qquad (3)$$

In the above equations r represents the opening radius at some arbitrary time t. R represents the initial radius of the diaphragm and T represents the total diaphragm opening time.

The diaphragm was also discretized into 30 segments. Initially all the diaphragm segments are considered to be wall and at each time step the segments are opened sequentially. The segments lengths were so chosen such that each segment opening results to the opening radius at that corresponding time. By this way the entire diaphragm opening process was simplified into a thirty discrete step opening process .Three different cases were considered with three different opening radius functions with respect to time as shown in Table.1

Table. 1 Initial conditions for different opening functions

Cases	Dia	P4/P1	P1 (Pa)	Opening Function
1	1 mm	100	292.35	Linear
2	1 mm	100	292.35	Cosine
3	1 mm	100	292.35	Quadratic

Different opening process has been shown in Fig.4.In the present study the actual continuous opening process has been replaced by discrete step opening process. As sufficient number of opening steps (30 steps) has been considered the piecewise step function will

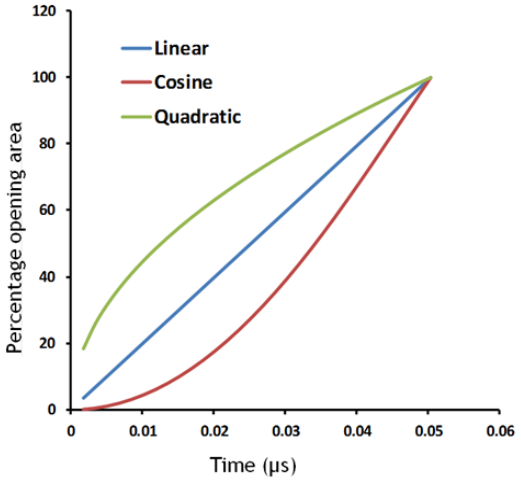

Fig. 4 Diaphragm opening area variation with respect to time based on different opening functions

nearly match the continuous function.

The flow physics was mathematically modeled using unsteady Reynolds Averaged Navier-Stokes equations. SST k-ω model was used to predict the turbulent eddies. Ideal gas behavior was considered for all the species and viscosity variation with respect to temperature was modeled using Sutherland viscosity model. The flux component of the governing equation was discretized using AUSM scheme. A second order implicit scheme was used for the temporal discretization. The extrapolation of cell centre values to the face centers was done using third order MUSCL schemes. The governing flow equations were solved in a coupled manner using commercial solver, Fluent. To account for the rarefaction effects which happen at low pressure Maxwell's slip velocity and temperature jump equations [10], as shown below, were employed. User defined functions [11] were used to input these equations to the solver and subsequent to each flow iteration the pre defined functions for slip conditions were called into the solver and executed to update the near wall fluid velocity and temperature.

$$U_w - U_g = \left(\frac{2-a_v}{a_v}\right)\frac{\lambda}{\delta}\left(U_g - U_c\right) \quad (4)$$

$$T_s - T_w = 2\left(\frac{2-a_T}{a_T}\right)\frac{\lambda}{\delta}\left(U_g - U_c\right) \quad (5)$$

$$\lambda = \frac{k_B T}{\sqrt{2}\,\pi\sigma^2 p} \quad (6)$$

Here the subscript g, c and w refer to gas, cell centre and wall quantities respectively. av and at are the momentum and thermal accommodation coefficients respectively.λis the molecular mean free path.

2.1 VALIDATION

The accuracy of different diaphragm opening functions was compared with the experimental results of Matsuo. In the experiment the expansion wave propagation has been monitored at 150 mm behind the diaphragm.

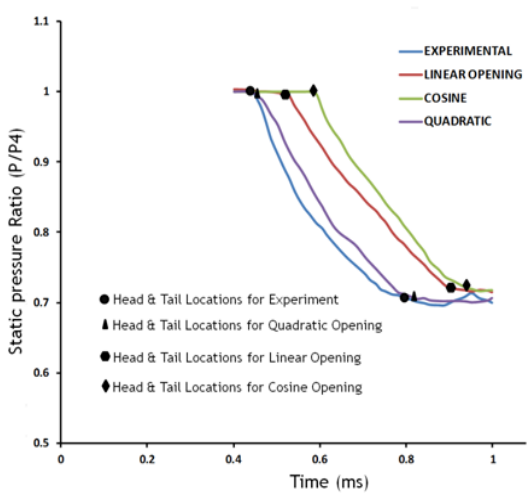

Fig. 5 Static pressure comparisons in the driver section for different cases at X/D=-2.29

Figure 5 shows the pressure value at the measuring point at various times. It can be

clearly noted that the quadratic function shows more closer results compared with the experimental values. The cosine opening function shows a considerable deviation from the experimental values and this may be due to the fact that for the cosine opening the initial rupture process is gradual and then it becomes rapid. Because of this the flow evolution takes more time for cosine opening process were as for quadratic opening function the opening area grows rapidly at the beginning and then slows down.

3. RESULTS AND DISCUSSION

As the diaphragm starts to open the high pressure fluid from the driver section escapes into the low pressure driven section. This results in a series of compression waves that eventually gets piled up and leads to a shock wave. So the shock front will be generated after a particular distance ahead of the diaphragm. The static temperature contours at various times for a quadratic opening process as shown in Fig.6 clearly explains this.

Figure 7 shows expansion head, contact and shock wave propagation inside the micro shock tube. The contact location was identified as the location where a sudden rise in temperature happens and shock position is the location where the temperature suddenly dips.

The ideal viscous shock tube equation explains that the shock strength will be a constant value. But in real situation this may not be the case due to viscous losses, finite diaphragm rupture process and turbulent losses. Because of the gradual opening consideration, a fully developed flow into the driven section takes some time. Due to this factor, the shock front will be generated after

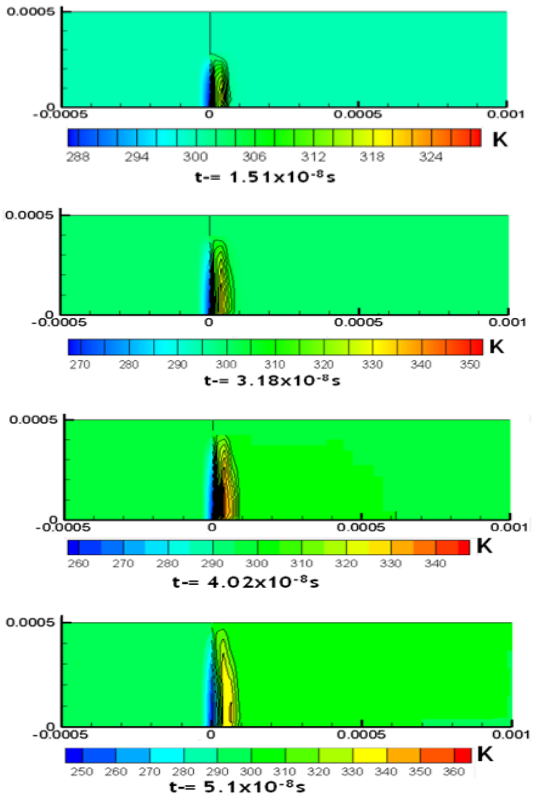

Fig. 6 Static temperature distributions in the driven section at different diaphragm opening stages

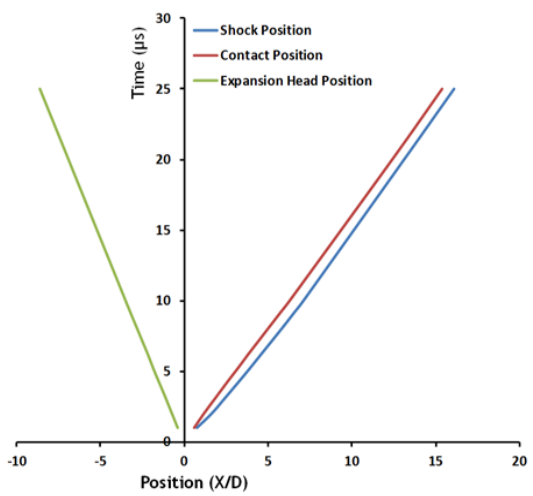

Fig. 7 Expansion, Contact and Shock wave propagation (x-t diagram) distances at various times

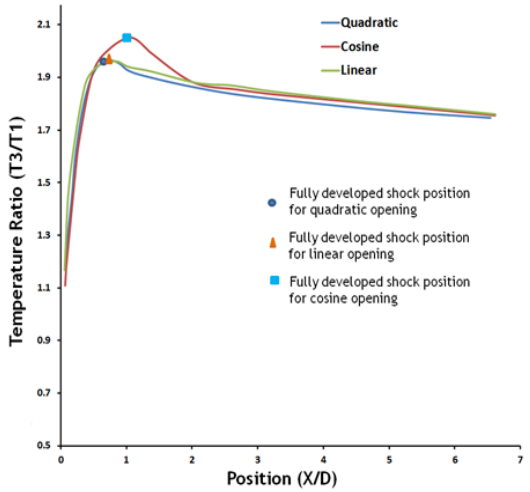

Fig.8. Temperature ratio distributions across the shock front along the axis under different opening conditions

some particular distance ahead of the diaphragm where as for a sudden rupture case an instantaneous production of shock front can be visualized. So for real situation the shock strength initially increases and then decreases. The temperature ratio across the shock is a direct indication for the shock strength and this is being compared along the length as shown in Fig.8

The fully developed shock position was determined as the location where the shock strength reaches its maximum value. It can be observed from Fig.8 that a fully developed shock front in the case of a cosine diaphragm opening function occurs at a larger distance from the diaphragm as compared with that of a quadratic opening. This can be attributed due to the fact that for quadratic function the opening process is much rapid in the beginning and then becomes gradual where as in the case of cosine opening this is just reverse process. The rapid opening of diaphragm at the beginning causes a much faster development of flow evolution there by producing a completely developed shock front at a much advanced distance compared with that of cosine opening model. Also the flow losses happening at the beginning will be higher for the case of quadratic opening process due to a higher flow rate and this result in a lesser temperature rise downstream of the shock for this case compared with the cosine opening case. The shock development distance for different opening functions is shown in Table.2

Table. 2 Shock development distance from diaphragm for various opening functions

Opening Function	Shock Formation distance from diaphragm
Linear	0.88 mm
Cosine	1.06 mm
Quadratic	0.74 mm

The shock propagation inside micro shock tube suffers much more attenuation in shock strength compared to macro shock tube flows. This is mainly because boundary layer thickness fills much of the core flow and produces more viscous losses. If the initial operating pressure is low then rarefaction effects happens and this changes the near wall flow field. This eventually alters the shock propagation phenomenon. At low pressure the boundary layer thickness increases and this also leads to much attenuation compared to a high operating pressure system. Three CFD simulations with sudden rupture conditions were carried out to simulate these effects as shown in the table. 3

The shock propagation distance along the distance as shown in Fig.9 clearly explains the attenuation phenomenon. It can be clearly

Table. 3 Initial conditions for studying the pressure dependency and slip effects on shock propagation

Cases	P4/P1	P1 (Pa)	Dia (mm)	Wall Conditions	Diaphragm Opening
A	15	500	2	No Slip	Sudden Rupture
B	15	50	2	No Slip	Sudden Rupture
C	15	50	2	Slip	Sudden Rupture

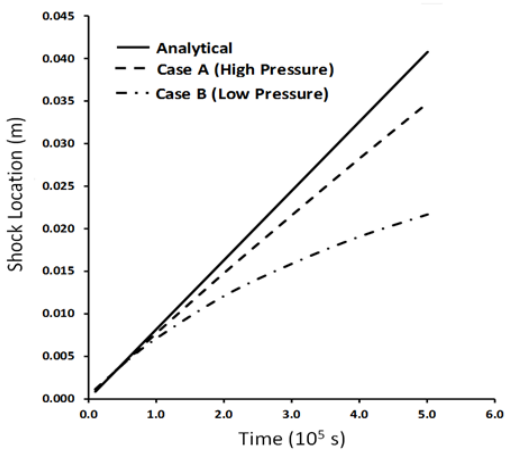

Fig.9. Shock location along axis (d=2mm) at different initial pressure conditions

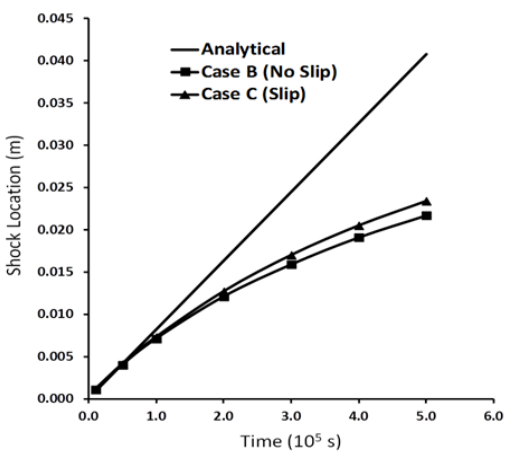

Fig.10. Shock location along axis (d=2mm) for slip and no slip case

noticed that the shock location for micro shock tube (Case A) clearly drags from the ideal analytical position. At low pressure (Case B) the attenuation effect will be more due to the larger boundary layer thickness producedThe consideration slip conditions (Case-C) introduces additional velocity and temperature jump to the wall attached fluid. This produced more pronounced core flow in the case of slip case flow and reduces the attenuation which can be observed from Fig.10.

4. CONCLUSION

In the present study the effect of diaphragm opening process on the shock evolution with three different opening functions (linear, cosine and quadratic functions) were numerically studied. The consideration of finite rupture time results in the development of fully developed shock front at certain distance ahead of the diaphragm. The shock development distance is minimum in the case of a quadratic opening function. The opening process will be rapid at the initial stages for quadratic opening function compared to other opening process and hence flow evolution will be faster for this case which results in less shock development distance. The shock strength initially increases to reach a maximum value and then decreases. This is because during the gradual opening process the flow evolution into the driven tube initially accelerates to a maximum point after which the flow viscous resistance dampens the shock Mach number. The shock propagation attenuates in the case of a micro shock tube compared to a macro shock tube. This is mainly because of the severe viscous losses associated with the boundary layer thickness

which will considerably affects the core flow due to very small flow diameter. As the driven section pressure reduces a thicker boundary layer forms compared to the high pressure case. This produces more loss in low pressure case and subsequently produces more attenuation to shock movement. The implementation of slip boundary condition on the walls to simulate the rarefaction effects reduces the losses produced and this eventually helps in shock propagation.

ACKNOWLEDGEMENT

This work was supported by the National Research Foundation of Korea (NRF) grant funded by the Korea government (MEST) (2011-0017506)

REFERENCES

1) Duff, R.E ., "Shock Tube performance at initial low pressure",Phys. Fluids ,Vol.4 , 1958,pp.207-216
2) Brouillette, M ., "Shock waves at microscales", Shock Wave ,Vol.13,2003,pp. 3-12
3) Zeitoun, D.E., Burtschell, Yves ., "Navier-Stokes computations in micro shock tubes", Shock Waves, Vol. 15, 2006, pp. 241-246
4) Zeitoun, D.E., Burtschell, Yves., Graur, I. A., Ivanov, M. S., Kudryavtsev, A. N., Bondar, Y. A., "Numerical simulation of shock wave propagation in micro channels using continuum and kinetic approaches", Shock Waves ,Vol.19, 2009, pp. 307-316
5) Shigeru Matsuo., Mamun Mohammad.,Shinya Nakano.,Toshiaki Srtoguchi.,Heuy Dong Kim., "Effect of a diaphragm rupture process on flow characteristics in a shock tube using dry cellophane", International Conference on Mechanical Engineering,December 2007
6) Outa, E., Tajima, K.,Hayakawa,K., "Shock tube flow influenced by diaphragm opening (two-dimensional flow near the diaphragm)",10th International Symposium on shock waves and Shock Tubes",1975
7) Rothkopf,E.M., Low,W., "Diaphragm opening process in shock tubes",Phys.Fluids,Vol.17,1974,pp.1169-1173
8) Mizoguchi,E.M., Aso,S., The effect of diaphragm opening time on the feasibility of tuned operation in free piston shock tunnels",Shock Waves,Vol.19,2009,pp.337-347
9) Roy, S.H., Larry, C.F., James, B.K ., " Behavior of burst diaphragm in shock tubes", Phys.Fluids,Vol.18,1975,pp.1249-1152
10) Karniadakis, G.E.M., Beskok, A., "Micro Flows fundamentals and Simulation",Springer,Berlin Heidelberg New York (2000)
11) Fluent user's guide manual, http://www.fluent.com/